Physio-climatic controls on vulnerability of watersheds to climate and land use change across the United States

Ankit Deshmukh,[1] Riddhi Singh[1]

Corresponding author: Ankit Deshmukh, Department of Civil Engineering, Indian Institute of Technology, Hyderabad, Kandi, Telangana, 502285, India. (deshmukh.iith@gmail.com)

[1]Department of Civil Engineering, Indian Institute of Technology, Hyderabad, Kandi, Telangana, 502285, India

Key Points.

Climate change, land use change, vulnerability, Bottom up approach, Hydrologic indicators, comparative hydrology

Abstract.

Understanding how a watershed's physio-climatic characteristics affect its vulnerability to environmental (climatic and land use) change is crucial for managing these complex systems. In this study, we combine the strengths of recently developed exploratory modelling frameworks and comparative hydrology to quantify the relationship between watershed's vulnerability and its physio-climatic characteristics. We propose a definition of vulnerability that can be used by a diverse range of water system managers and is useful in the presence of large uncertainties in drivers of environmental change. This definition is related to adverse climate change and land use thresholds that are quantified using a recently developed exploratory modelling approach. In this way, we estimate the vulnerability of 69 watersheds in the United States to climate and land use change. We explore definitions of vulnerability that describe average or extreme flow conditions, as well as others that are relevant from the point of view of instream organisms. In order to understand the dominant controls on vulnerability, we correlate these indices with watershed's characteristics describing its topography, geology, drainage, climate, and land use. We find that mean annual flow is more vulnerable to reductions in precipitation in watersheds with lower average soil permeability, lower baseflow index, lower forest cover, higher topographical wetness index, and

vice-versa. Our results also indicate a potential mediation of climate change impacts by regional groundwater systems. By developing such relationships across a large range of watersheds, such information can potentially be used to assess the vulnerability of ungauged watersheds to uncertain environmental change.

1. Introduction

1.1. Towards vulnerability based approaches for managing change in water resources

Quantifying the hydrologic response of a watershed to changing climate and land use is essential for managing the water dependent ecological and economic systems in a region. There are now a plethora of studies that attempt to obtain the projections of water resources under changing climate at various spatial and temporal scales [*Vörösmarty et al.*, 2000; *Legesse et al.*, 2003; *Arnell*, 2004; *Sun et al.*, 2008; *Anandhi et al.*, 2015; *Watts et al.*, 2015; *Henderson et al.*, 2015; *Chen et al.*, 2015]. Many efforts in this direction have culminated in the understanding that future water resources projections are ultimately dependent upon the projections of the drivers of change (land use and climate change), the type of hydrologic model used, parameter identification strategies adopted, and several such subjective decisions that are made while using the hydro-climatic chain [*Wood et al.*, 2004; *Tebaldi et al.*, 2005; *Hidalgo et al.*, 2008; *Dobler et al.*, 2012; *Bosshard et al.*, 2013; *Addor et al.*, 2015; *Giuntoli et al.*, 2015; *Vetter et al.*, 2015].

Typically, the resultant uncertainties in projections tend to be larger than the required precision of these projections for planning purposes [*Schewe et al.*, 2014; *Singh et al.*, 2014a]. The presence of such large uncertainties warrants a shift in focus of problems formulated for climate change adaptation from obtaining projections to understanding what makes a watershed vulnerable to environmental change. This type of assessment first requires a definition of vulnerability that allows its quantification based on streamflow, climate, and land use change data. Literature provides some guidelines as to how to formulate such a definition. For example, *Chatterjee et al.* [2014] classify the ranges of soil

erosion (expressed in tonnes per hectares per year) into various erosion vulnerability units (EVUs) (or classes) in order to quantify historical levels of erosion vulnerability in their study area. *Fraser et al.* [2013] define vulnerability hotspots for cereal production as those regions where an integrated socio-economic and hydrologic modelling framework projects a likely decline in adaptive capacity as well as available soil moisture. *Klein et al.* [2014] quantify vulnerability of trees to drought as the probability that vapor pressure deficit reaches or remains below a critical threshold. *Van Vliet et al.* [2012] define vulnerability of power plants across the Europe and United States to climate change based on the decreases in their usable capacity. Thus, quantification of vulnerability varies with the type of indicator being analysed and the context of the analysis.

Here, we define vulnerability as threshold of environmental change that leads to deterioration in a hydrologic indicator related to hydrologic, ecologic, or socio-economic impacts. Thus, vulnerability is always directly related to adverse impacts, and to decision makers' preferences and pre-existing norms. It is also worth noting here that vulnerability as defined here is a broader term when compared to climate elasticity, an often utilized measure to quantify impacts of environmental change on water resources [*Schaake and Liu*, 1989; *Nash and Gleick*, 1991; *Sankarasubramanian et al.*, 2001; *Renner et al.*, 2012; *Johnson et al.*, 2015]. Climate elasticity of streamflow is the relative change in streamflow for a unit change in an environmental metric [*Schaake and Liu*, 1989]. Climate elasticity of streamflow is generally used to infer long term hydrologic changes and is likely to be nonlinearly related to changes in other hydrologic indicators such as those describing hydrologic extremes, or survivability of instream organisms.

We propose a modelling based framework to quantify vulnerability using existing information about a watershed's hydrologic and physio-climatic characteristics. This allows the decision maker to guide the modelling process based on their perception of ranges of a hydrologic indicator that are acceptable [*Rougé et al.*, 2015]. We build upon recently developed bottom–up or exploratory modelling approaches to build this framework [*Bankes*, 1993; *Lempert et al.*, 2008; *Brown et al.*, 2011, 2012; *Boso et al.*, 2013; *Khader et al.*, 2013; *Kunreuther et al.*, 2013; *Moody and Brown*, 2013; *Weaver et al.*, 2013; *Poff et al.*, 2015]. *Brown and Wilby* [2012] and *Nazemi and Wheater* [2014] summarize two modelling paradigms that are generally used to estimate the impact of environmental change on hydrologic response of a watershed. One approach forces a hydrologic model using available climate or land use change information. For example, climate change data from downscaled global climate models is used to force a hydrologic model calibrated on historical streamflow data. The alternative, bottom-up approach, explores a large space of possible environmental changes to identify those that are likely to lead to deterioration in an indicator of interest.

Bottom-up or exploratory modelling approaches employ a hydrologic model to assess the response of a watershed to a large range of artificially applied changes in climate and land use. Then, the relative change in hydrologic indicators of interest as compared to their historical values are estimated for each change scenario. The simulated change in these indicators can then be classified as vulnerable or otherwise. A multi-tier classification is also possible [*Singh et al.*, 2014a]. Finally, by using appropriate search algorithms, the thresholds of change in climate and land use that lead to vulnerability can be estimated. We propose a new method to estimate these thresholds using the information provided by

the exploratory modelling framework developed by [*Singh et al.*, 2014a]. In this way, we quantify vulnerability indices as maximum tolerable climate or land use changes beyond which the value of a chosen hydrologic indicator is classified as vulnerable. We use a range of hydrologic indicators, those that characterize economic as well as ecologic health of a region.

1.2. Relating vulnerability to watershed characteristics

For a thorough understanding of watershed's potential response to change, the link between its vulnerability and physio-climatic characteristics needs to be explored. *Berghuijs et al.* [2016] relate relative changes in streamflow to changes in watershed storage by using streamflow data for a large number of watersheds across Europe. They found that high flow variability tends to be increase the sensitivity of streamflow to changes in watershed storage. *Stewart* [2013] relates physical watershed characteristics to climate elasticity of California mountain streams and reveal that elevation is related to climate elasticity. They find that differences in climate elasticity can be explained by differences in elevation ranges along with combinations of physical watershed characteristics. There are two ways in which such relationships between a vulnerability metric and watershed physio-climatic characteristics can be further generalized. First, decision makers are most likely to be interested in a flexible vulnerability metric that can incorporate their own definitions of adverse impacts. We enable this by adopting a modelling based framework to assess vulnerability. Second, the relationship between watershed's physio–climatic characteristics and its vulnerability should be explored across a larger range of watersheds and environmental changes, which should help to identify transferable generalizations. We achieve

this goal by combining the strengths of comparative hydrology and exploratory modelling framework.

Comparative hydrology when applied in conjunction with the exploratory modelling framework can aid in identifying the dominant controls on watersheds' vulnerability to change. Comparative hydrology attempts to understand the interactions between streamflow response, and its physio-climatic drivers across a large range of watersheds, and also helps to determines the extent to which hydrologic predictions may be transferred from one area to another [*Falkenmark et al.*, 1989]. It advances hydrologic theory by identifying generalizable patterns across a large number of watersheds [*Blöschl*, 2006; *Sivapalan*, 2009]. Examples where comparative hydrology has provided significant insights in hydrologic theory include prediction in ungauged basins [*Blöschl*, 2013]. In the presence of complete information about the relationship between a watershed's hydrologic response and its physio-climatic characteristics, we can potentially relate each vulnerability metric to different physio-climatic characteristics purely based on physical understanding. This is of course challenging due to the various complexities and interactions inherent in hydrologic processes. However, the proposed model based approach to quantify vulnerability of a watershed to climate or land use change can be easily applied across a large range of watersheds to assess whether there is any relationship between these vulnerability indices and watershed's physio-climatic characteristics.

In this study, our main contribution is to define a model based metrics of vulnerability and link them to watershed physio-climatic characteristics for a large number of watersheds across the conterminous US. We quantify watershed vulnerability to environmental change by extending the exploratory modelling framework developed by *Singh et al.*

[2014a]. We then relate the vulnerability metric with watershed physio-climatic characteristics in order to assess important controls on watersheds' vulnerability to change. We select watersheds with a significant hydro-climatic gradient in order to perform the comparative analysis. The exploratory modelling analysis simulates watershed's dynamic response to a large number of climate and land use change combinations, using which we quantify various hydrologic indicators that determine water availability in the region, occurrence of flood and droughts, and also the survivability of instream organisms. We then determine the critical thresholds of climate and land use change for each indicator, which are the vulnerability metrics employed in this study. Finally, we quantify the relationship between watersheds' vulnerability to climate and land use change and its physio-climatic characteristics. This allows us to identify characteristics that make a watershed more or less vulnerable to changing climate or land use.

2. Methodology

2.1. Modelling framework

We adopt the exploratory modelling framework proposed by *Singh et al.* [2014a] with modifications in the method for parameter uncertainty quantification (Figure 1). We begin by defining feasible ranges of climate and land use change as shown by the uncolored cube in the left side of Figure 1a. We sample within this feasible space to generate several scenarios of change. These climate and land use changes are then propagated through a hydrologic model that incorporates parametric uncertainties. In this way, the total number of streamflow simulations, N, explored for each watershed can be estimated as:

$$N = P \times T \times L \times \Theta$$

where, P is the number of precipitation change scenarios, T is the number of temperature change scenarios, L is the number of land use change scenarios, and Θ is the number of parameter sets considered. Next, we estimate the hydrologic indicators of interest for each streamflow simulation. Once the indicators are estimated, their values are classified into different classes based on pre-specified thresholds. Following this, classification and regression trees (CART) identify the regions in the input space that lead to vulnerable classes. This provides a way to estimate the critical values of climate and land use changes that lead to vulnerability. For example, in Figure 1a, an indicator is classified into four classes (each class represented with a color) and using CART, the climate and land use combinations that lead to vulnerability can be determined.

Once the critical thresholds of climate and land use change for each watershed-hydrologic indicator combination are obtained, we employ the comparative hydrology approach to find the relationship between vulnerability of the indicator (represented by the critical change thresholds) and watershed physio-climatic characteristics (Figure 1b). This allows us to assess the likely controls exerted by watershed's characteristics on its vulnerability to climate and land use change. To apply the comparative hydrology approach, we correlate critical thresholds of precipitation and land use change with watersheds physio-climatic characteristics such as those that represent drainage, topography, geology, land use, and climate.

2.2. Hydrologic model

We use a spatially lumped form of a parsimonious rainfall runoff model that simulates streamflow at daily time steps (Figure 2). The model has a basic representation of land use in the form of percent of deep rooted vegetation that can be altered to simulate

land use change. The model structure is adopted from parsimonious structures suggested by *Farmer et al.* [2003], and used further by *Bai et al.* [2009]. The model comprises of a snow module, a soil moisture accounting module, and a routing module. The snow module is based on the degree-day method that uses three parameters to estimate snow storage and melt. The snow module takes in daily precipitation and provides fluxes of daily melt and rainfall, which are then passed on to the soil moisture accounting (SMA) module. The SMA module comprises of multiple buckets in parallel configuration, and employs the saturation excess mechanism of fill and spill to generate effective rainfall [*Zhao and Zhang*, 1980; *Bai et al.*, 2009]. Evapotranspiration is also estimated in SMA based on parameters that determine the leaf area index and percentage of deep rooted vegetation cover, with impact of phenology adopted from *Sawicz* [2013]. The land use parameter divides the watershed area into bare soil and deep rooted vegetation cover, and evapotranspiration over each is estimated separately [*Farmer et al.*, 2003]. For more details, readers are referred to *Singh et al.* [2014a]. The model has a total 13 parameters including one representing land use (Table 1).

2.2.1. Identification of parameter ranges and behavioural parameter sets

Parametric uncertainty is incorporated in the analysis using a three step process for uncertainty quantification (Figure 3). We begin with a literature survey to identify the feasible range of each parameter. Then, we compute *a priori* parameter ranges for six parameters and others are fixed at their full range (Table 1) [*Farmer et al.*, 2003; *van Werkhoven et al.*, 2008; *Bai et al.*, 2009; *Kollat et al.*, 2012; *Singh et al.*, 2014a]. *A priori* parameter ranges are estimated in two ways: soil and phenology related parameters (S_b, F_c, LAI_{min}, LAI_{max}) are estimated using observed physical characteristics of watersheds

obtained from Falcone database while recession parameters (A_{SS}, A_{BF}) are obtained using recession curve analysis based on historical streamflow data (See *Singh et al.* [2014a] for more details). *A priori* ranges of parameters for each watershed are listed in supplementary material Table S1.

Next, we generate 50,000 parameter sets using latin hypercube sampling method by assuming uniform distribution of parameters within *a priori* ranges. We further constrain these parameter sets by testing their ability to reproduce magnitude and variability of historically observed streamflow, quantified through Nash Sutcliffe efficiency (NSE) and volumetric bias. Parameter sets producing NSE greater than 0 and percentage volumetric bias within 25% are accepted as behavioural. Finally, best 50 sets based on NSE performance (or all producing positive NSE) are used to simulate watershed response.

2.3. Hydrologic indicators for vulnerability assessment

We select four indicators that represent average water availability, hydrologic extremes (floods and droughts) and health of instream organisms (Table 2). This choice of indicators is governed by the need to capture both economic and ecologic aspects of the services provided by streams. The selected indicators are – mean annual flow, frequency of floods, streamflow drought index, and proportion of index flow removed. Definition for flood frequency and streamflow drought index are adopted from *Olden and Poff* [2003] and *Nalbantis and Tsakiris* [2009], respectively. The streamflow drought index (SDI) is based on the cumulative volume of streamflow for overlapping period of three, six, nine, and twelve months within a hydrologic year [*Nalbantis and Tsakiris*, 2009]. The index flow removed (IQ_{dsc}), specified as reductions in median August discharge divided by the mean

annual discharge, has been related to fish populations by a variety of previous studies [*Ries*, 1997; *Poff et al.*, 2010].

For assigning indicator values to classes, we use literature based class definitions of vulnerability wherever available, or adopt a classification based on the relative change in indicator magnitude for a scenario compared to its historically observed value. Based on the assumption that mean annual flow is a proxy for water availability in a watershed, it is assumed to become vulnerable if its values fall below historically observed values. Once the values decrease beyond a threshold, the vulnerability class is changed. In this way, four vulnerability classes are defined for mean annual runoff. Reductions in mean annual runoff as compared to historical value are classified into C1, C2, or C3, with each class spanning a range of successive 25% reductions. Increases in mean annual runoff are assigned class C0. Similarly, we classify frequency of flooding into four classes. Successive relative increases are assigned to classes C1, C2, and C3 while decreases are assigned to C0 (Table 2). For IQ_{dsc} and drought indicator, we use pre-defined class definitions from past literature. The drought indicator is classified into five classes (C0–C4) based on the probability of occurrence of categorized SDI values with C0 to C4 representing increasing drought conditions [*Nalbantis and Tsakiris*, 2009]. Class definition for IQ_{dsc} are adopted from *Poff et al.* [2010], who classify IQ_{dsc} into three classes – C0, C1, and C2, each class related to a reduction of 0%–10%, 10%–30%, and >30% in fish population, respectively. Thus across all indicators, C0 to C4 represent an increasing level of vulnerability.

2.4. Threshold identification via classification and regression trees (CART)

Each indicator class is a result of possible combinations of climate change, land use, and parameter sets. Classification and regression trees (CART) allow us to identify the space

of climate, land use and hydrologic model parameters that lead to vulnerable classes of indicators. CART is a binary recursive partitioning algorithm that divides multiple variable input space into subspaces and each subspace is related to an output indicator class [*Breiman et al.*, 1984]. To implement CART, we use the statistical classification and regression tree package in R, "rpart" [*Therneau et al.*, 2010]. 'rpart' also performs a tenfold cross validation of the CART output to ensure that the final structure of the trees is not over-fitted to the data. The output of CART provides a series of logical yes/no type decisions such that the input space that results in a certain class of indicators is identified. In this way, critical thresholds for a watershed are estimated as the values of climate (precipitation and temperature) change or land use that lead to a vulnerable class for a given hydrologic indicator.

3. Study area and data

We implement the CART analysis to identify critical thresholds for climate change and land use across 77 watersheds in the conterminous United States (Figure 4). The hydro meteorological data sets used in this study were developed as part of the Model Parameter Estimation Experiment (MOPEX) [*Duan et al.*, 2006]. These watersheds represent the largest set of reference watersheds from the MOPEX database with an overlapping period of 10 years for the streamflow data from 1959-1968 [*Singh et al.*, 2014b]. Reference watersheds are classified as minimally impacted in the Falcone database based on three criteria: a quantitative index of anthropogenic modification within the watershed based on GIS derived variables, visual inspection of every stream gage and drainage basin from recent high resolution imagery and topographic maps, and information about man-made influences from USGS Annual Water Data Reports [*Falcone et al.*, 2010]. A summary of

watershed related information is provided in supplementary material Table S2. Watershed characteristics for correlation analysis and *a priori* parameter identification are obtained from the Falcone database [*Falcone et al.*, 2010].

4. Results

We begin the presentation of results with the implementation details of the exploratory modelling framework (Section 4.1) such as the sampling of climate and land use scenarios (Section 4.1.1), and the method for estimation of critical thresholds (Section 4.1.2). This is followed by the first main result - the spatial mapping of vulnerability of watersheds to climate and land use change for mean annual flow across US (Section 4.1.3). We then move on to the application of the comparative hydrology approach to explore the relationships between watershed physio-climatic characteristics and their quantified vulnerabilities (Section 4.2).

4.1. The exploratory modelling framework

4.1.1. Sampling of climate and land use scenarios

To generate the climate scenarios, we use the delta change method in which mean of climate variables (precipitation and temperature) are changed keeping higher order moments fixed. The delta change method is generally used in the context of downscaling to refer to the process that applies projected differences in temperature or precipitation from Regional Climate Models (RCMs) to historical climate data to obtain future climate trajectories [*Teutschbein and Seibert*, 2012]. Precipitation scenarios are generated by varying the precipitation time series within -40% to +60% of their historical values, and temperature change scenarios are generated by adding 0 °C to 12 °C of temperature increases to

the historical temperature time series. The precipitation and temperature change values are selected such that they are wide enough to incorporate the maximum change over a long time period as reported in the fifth assessment report of the International Panel for Climate Change [*Van Oldenborgh et al.*, 2013]. Scenarios of land use change are generated by sampling the land use related parameter in the hydrologic model between 0–1 (completely bare soils to full vegetation cover). Precipitation, temperature, and land use changes are applied in increments of 10%, 1 °C, and 0.1, respectively. This results in 1859 combinations of potential climate and land use changes ($13 \times 13 \times 11$). Each scenario is further combined with uncertain hydrologic model parameters. In this manner, we end up with a maximum of 92,950 (1859 x 50) combinations of climate, land use, and parameter sets for each watershed. Note that for watershed USGS gauge ID:011355500, we are unable to identify any parameter set that satisfies the performance criteria. In addition, we found seven watersheds with runoff ratio less than 0.1 in the historical climate. As the hydrologic model employed in this analysis is not likely to represent the hydrologic processes in these semi-arid watersheds adequately, we exclude them from further analysis. This reduces the total number of watersheds we analyse to 69.

4.1.2. Identification of critical thresholds

Once we identify the ranges for climate and land use change along with uncertainty estimates for hydrologic model parameters, we run the hydrologic model to simulate the streamflow and estimate the hydrologic indicators of interest for each combination. This is followed by categorization of these indicators based on predefined class definitions. Then, CART is used to partition the input space of climate, land use, and parameters to identify

regions that lead to vulnerable values of the hydrologic indicator and estimate the critical values of climate and land use change.

A typical output from CART analysis for War Eagle Creek watershed near Hindsville, AR, USGS gauge ID 07049000, is shown in Figure 5. The figure outlines the process of estimating the critical values of precipitation change that lead to vulnerable class C3 for mean annual runoff for this watershed. We term this value *the critical precipitation change threshold* for mean annual runoff to transition to C3. We begin by identifying all leaf (end) nodes that result in a vulnerable class (C3). Following this, the values of precipitation change that lead to C3 class are noted along with the total number of scenarios that belong to each end node. Finally, the critical threshold is calculated as the weighted average of precipitation change values resulting in the end nodes with the vulnerable class, using the number of scenarios of each end node as weights. For the example watershed in Figure 5, the critical precipitation change threshold estimate turns out to be 0.757. Note that this value is expressed as a multiplier on the historical precipitation and represents a 24.3% reduction in precipitation. We thus conclude that if mean annual precipitation falls below this threshold, the mean annual runoff is likely to transition to a vulnerable regime, which in this case represents a reduction in mean annual flow of greater than 50% of the historical value.

The values of critical precipitation change threshold close to unity indicate a more vulnerable watershed for mean annual runoff. For example, if two watersheds have a critical precipitation change threshold of 0.6, and 0.9, respectively, the second watershed is more vulnerable to climate change for mean annual runoff. This is because a smaller reduction in mean annual precipitation would be required to cause this watershed to transition to

a vulnerable regime. We also found that temperature appeared in the CART output less frequently than precipitation and thus focus on results for the critical precipitation change threshold across watersheds.

The critical land use threshold is estimated as 0.55 from Figure 5 on similar lines. This number is the fraction of deep-rooted vegetation cover in the watershed above which mean annual runoff transitions to a vulnerable regime. Recall that the land use parameter is varied from 0 to 1 (bare soils to full coverage of deep-rooted vegetation). Thus a land use threshold of 0.55 implies that if more than 55% of the watershed is covered by deep rooted vegetation, the increased evapotranspiration is likely to reduce the mean annual runoff by more than 50% thereby leading towards a transition to the vulnerable class. It is important to stress here that this land use threshold is applicable only for the range of precipitation changes (15% to 25% reductions) that lead to the node containing land use change as the split parameter.

4.1.3. Threshold mapping

Here we discuss the spatial variability of critical precipitation change and land use thresholds for mean annual runoff that is a proxy for the overall water availability in the watersheds (Figures 6 & 7). Figure 6 shows the critical precipitation change threshold obtained for each watershed. The threshold denotes the reduction in long term precipitation that causes a transition to the vulnerable class, C3. Increasing size of circles also indicates increasing vulnerability as value closer to 1 are more vulnerable. The variation of aridity indices are shown via color variation in the figure as previous studies have shown that it tends to impact watershed's sensitivity to climate change [*van Werkhoven et al.*, 2008; *Singh et al.*, 2011]. Our results too indicate that watersheds with lower aridity index

tends to be less vulnerable to precipitation change and vice versa (Figure 6). The spatial patterns also emphasize that watersheds in close proximity can also have significantly different critical precipitation thresholds.

We show the spatial variation of these land use thresholds in Figure 7. Note that in our model, land use change implies conversion between vegetated surface and bare soils, and only affects the evapotranspiration process. We find that 4, 6, 21, and 9 watersheds display land use threshold range of 0.25–0.35, 0.35–0.45, 0.45–0.55, and 0.55–0.65, respectively. A higher value suggests that larger watershed area can be covered by vegetated surfaces, while preventing mean annual runoff to transition to class C3. We also notice that watersheds with lower aridity index tend to have lower critical land use thresholds (correlation coefficient of 0.39 at significance level < 0.05).

4.2. Comparative hydrology analysis

In order to identify the physio-climatic controls on watersheds' vulnerability to environmental change, the estimated critical thresholds for all indicators are correlated with watershed characteristics. We consider several drainage, topographical, geological, and land use characteristics for each watershed. We use a reduced list identified by *Singh et al.* [2014b] after analyzing a large set of characteristics in the Falcone dataset [*Falcone et al.*, 2010]. A total 17 characteristics are used – five drainage (topographic wetness index(TWI), % of 1^{st}, 2^{nd}, and 4^{th} order streams, stream density), four topographical (elevation, area, aspect eastness and northness), five geological (average permeability, average water table depth, % of soils belonging to hydrologic group B, % of silt and organic matter), and three land use characteristics (% agriculture, forest, and urban land). We also consider three climatic characteristics in our analysis – mean annual precipitation,

mean annual potential evapotranspiration, and aridity index. Using these physio–climatic characteristics, we quantify the correlation between each characteristic and critical precipitation change and land use thresholds for the four indicators (Figure 8). Scatter plots between critical thresholds and watershed characteristics are presented in supplementary material Figures S1 & S2.

For mean annual runoff, we find that TWI is positively correlated with critical precipitation change threshold (Figure 8a). This indicates that watersheds with high TWI are more likely to transition to vulnerable regimes even for small relative reductions in precipitation. Figure 8a also shows that increasing values of elevation, average permeability, depth to regional water table, percentage of forests, and long term mean annual precipitation are related to decreasing vulnerability of watershed to precipitation reductions. On the other hand, the critical precipitation change thresholds for flood frequency indicator is positively correlated with depth to regional water depth and percentage of soils belonging to hydrologic group B. This indicates that higher values of these characteristics leads to lower vulnerability for flooding. Note that the relationship between type of correlation (positive or negative) and vulnerability (higher or lower) is different for mean annual runoff and flood frequency. For mean annual runoff, the thresholds from CART output represent precipitation decreases that should not be reduced further, while for flood frequency, they represent precipitation increases that cannot be exceeded. The threshold interpretation for the drought indicator and IQ_{dsc} is the same as that for mean annual runoff.

In case of the drought indicator, TWI and mean annual potential evapotranspiration are negatively correlated with the critical precipitation change threshold. This indicates

an increase in the values of these characteristics likely increases the susceptibility of the watershed to droughts for even small decreases in precipitation. However, elevation is positively correlated with critical precipitation change threshold for the drought indicator. Thus for watersheds considered in this analysis, those at higher elevation are more likely to transition to a drought prone regime with small decreases in mean annual precipitation. The vulnerability of IQ_{dsc} only showed significant relationship with soil properties (percentage of soils belonging to hydrologic group B, and organic matter content). However, even these relationships show high scatter (Figure S1). Note that for this indicator we neglect two characteristics despite significant correlations as their scatter plots indicate that outliers are causing spurious correlations (Figure S1).

The critical land use thresholds for mean annual runoff show a small positive but significant correlation with aridity index (Figure 8b). In addition, we also find that land use parameter emerges as a significant control on mean annual runoff only for watersheds with aridity index < 1.4 (Figures S1 & S2). Among these watersheds, the identified thresholds generally increase with increasing aridity index, although a high scatter is observed (Figure S2). For IQ_{dsc}, only one property emerged as significant when correlating the critical land use threshold – the percentage of land use covered by forests. For the drought indicator, all three land use characteristics considered (percentage of land use belonging to urban, forest, and agriculture areas) are significantly correlated with the critical land use threshold. The percentage of urban and agricultural land use are positively correlated with critical land use threshold while percentage of forested land use is negatively correlated. We did not find any significant correlation between the watershed characteristics and critical land use thresholds for the flood frequency indicator. Although land use

change does effect the frequency of flooding [*Brath et al.*, 2006; *Reynard et al.*, 2001], our parsimonious conceptual model likely misses the spatial heterogeneity that is required to capture these effects.

4.2.1. Hierarchy of controls on watershed vulnerability

The CART output provides another source of information regarding the control of watershed characteristics on critical climate or land use thresholds. Each tree presents a hierarchy of controls for an indicator-watershed combination. This information can help in diagnosing the relative importance of climate, land use, and model parameterization in determining watershed's vulnerability to environmental change. Visualizing the outputs of all 69 trees would be challenging, so here we resort to Circos diagrams for high dimensional data visualization (Figure 9) (see also *Kelleher et al.* [2013]). Ranking of controls is determined for each indicator across all watersheds based on the hierarchy of controls from the CART output. For example, if CART output's first node is change in precipitation, we assign change in precipitation as primary control for that particular indicator-watershed combination. Similarly, we determine secondary, tertiary, and higher order controls. Thus, primary splits are assumed to have a higher impact on watershed vulnerability as they provide maximum information gain while splitting the space of indicator responses [*Breiman et al.*, 1984].

Following the method mentioned above, the controls for each indicator are plotted in separate chord diagrams created by the Circos tool developed by *Krzywinski et al.* [2009] (Figure 9). Circos uses a circular ideogram layout to facilitate the display of the relationships between a pair of variables represented through their position on a circle, and by the use of ribbons or chords. On the outer periphery of the circles in the Circos

diagram, we present controls (sky blue) and watersheds (black) considered in study. Each CART output is a result of varying the climate and land use in the watershed in the presence of parametric uncertainties. Thus, we consider six controls: precipitation change, temperature change, land use change represented by a model parameter, followed by parameters related to snow, soil, and routing, respectively. A total of 69 watersheds are shown in the chord diagram. The color of strips inside the circle represent the order of splits as obtained from the CART output.

For mean annual runoff, all watersheds show precipitation change on the primary as well as secondary split indicating that it is a main control on mean water availability in a basin. A few watersheds have land use change on their secondary splits and several have it on their tertiary split, indicating that it is the second most important control on this indicator. The impact of hydrologic model parameters related to snow, soil and routing, have negligible impact on mean annual runoff in the presence of large precipitation and land use change scenarios tested here. A small number of watersheds also show temperature as the tertiary control.

As opposed to mean annual runoff, the flood indicator shows a far more diverse range of controls. Precipitation is a dominating control for this indicator too, but here land use change emerges as a primary control for a significant number of watersheds. Hydrologic model parameters related to soil and routing emerge as tertiary controls for several watersheds. We can also find snow related parameters appearing as secondary and tertiary controls for a significant number of watersheds. We hypothesize that this is likely due to the role of snow melt in inducing flood response for some watersheds. Overall, we find that the controls on flood indicator are very complex. The IQ_{dsc} and drought indicators

are related to low flow and show similar controls. From their Circos diagrams, we find that the primary control on these indicators is precipitation change followed by land use change. For IQ_{dsc}, hydrologic parameters related to soils and routing are also significant. IQ_{dsc} seems to be more affected by land use change than the drought indicator as indicated by the higher number of watersheds showing land use change as a secondary indicator for IQ_{dsc}.

5. Discussion

In this study, we attempt to identify the dominant controls on watershed's vulnerability to environmental change. Vulnerability is defined using multiple indicators that act as a proxy for water availability, hydrologic extremes, and health of instream organisms. We assess the impact of watershed physio–climatic characteristics on its response to environmental change in two ways. We identify the watershed characteristics that are most correlated with the vulnerability index of an indicator (Figure 8). In addition, we also identify important controls on an indicator using the CART analysis (Figure 9). Here, we discuss our results using both these interpretations for each indicator.

For mean annual runoff, we find that watersheds in arid climates can transition to a vulnerable regime (<50% streamflow) for relatively small changes in mean annual precipitation (precipitation threshold >0.8) (Figure 8). Several studies have reached similar conclusions [*van Werkhoven et al.*, 2008; *Singh et al.*, 2011; *Gupta et al.*, 2015; *Sankarasubramanian et al.*, 2001]. We also observe that TWI emerges as an important control on vulnerability of mean annual runoff to precipitation change, with higher values related to higher vulnerability. First introduced by *Beven and Kirkby* [1979], TWI is computed as *ln(a/tan b)*, where a is the contributing area to a given site, and b is the local slope

angle at that site. Thus TWI increases as contributing area increases and slope angle decreases. High values of TWI have been associated with low mean transit times of baseflow in a basin [*Asano and Uchida*, 2012]. Thus, watersheds with quick responding or flashy streamflow are more likely to be vulnerable to reductions in precipitation. These results may also indicate that watersheds where water spends more time in a sub-surface storage are more robust to changing climate.

To test this hypothesis further, we estimated the correlation between baseflow index (BFI) and TWI across watersheds and found that both variables are indeed significantly correlated (-0.62, p-value <0.001). We also found BFI to be significantly correlated with watershed characteristics that were related to vulnerability of mean annual runoff to precipitation change (Figure 8a). However, BFI was found to be independent of the mean annual precipitation and aridity index (PE/P). Increasing drainage area should increase groundwater contributions, and decreasing slope angle should reduce the rate of groundwater transmission, assuming that surface topography approximates the hydraulic gradient for shallow groundwater systems [*Price*, 2011]. Thus overall, our results suggest that groundwater mediation plays a significant role in reducing vulnerability of watersheds to climate change.

We found that mean water availability is affected more by changes in mean annual precipitation than land use for all watersheds (Figure 9). However, land use change does emerge as an important second order control on mean annual streamflow for 58 out of 69 watersheds studied here. Moreover, for 19 watersheds, land use change emerges as more important than temperature change to classify mean annual streamflow. Other analysis based on observations of climate, streamflow, and land use change also suggest

that while both factors are important to explain changes in mean annual streamflow, generally precipitation change is more dominating. For example, *Schilling* [2016] show that precipitation change explains nearly 70% of changes in streamflow change a watershed in the Upper Mississippi River Basin, while the remaining changes can be attributed to land use change and other secondary factors. Another analysis by *Schottler et al.* [2014] showed that changes in both climate and land use are necessary to explain the observed increases in streamflow across 21 watersheds in Minnesota, US. A recent analysis by *Gupta et al.* [2015] shows that precipitation increase is more important than land use change for explaining the increased streamflow across 29 watersheds of Upper Midwest US.

For the flood indicator, we find that basins with greater extent of soil type belonging to hydrologic group B and lower depth to water table are less vulnerable to flooding (Figure 8). *Brutsaert* [1993] have shown that depth to the water table can be a measure of the initial storage capacity of a basin. This lends some physical basis for our results pertaining to the correlation of depth to water table and flood vulnerability since basins with low available storage will have lesser infiltration and more floods. In addition, *Kalantari et al.* [2014] also indicate that extent of urban areas, and soil type influences flooding.

In the context of ecology related indicator (IQ_{dsc}), our analysis suggests that greater coverage of soil belonging to hydrologic group B and higher organic content in soils generally lowers the vulnerability of IQ_{dsc}. Note that we do not consider the significant correlations for percentage of 4^{th} order stream and mean annual precipitation, as the scatter plots reveal that a single outlier is likely controlling the correlation (supplementary material Figure S1). Recall that we define this indicator on the basis of median August flow in seasonal flow. IQ_{dsc} simulates reduction in August median flow (late summer conditions

and low flow magnitude) and provides a measure of habitat availability during summer period [*Richter et al.*, 1996].

For the drought indicator, the comparative hydrologic analysis indicates that elevation and TWI are significantly correlated with the critical threshold of precipitation change (Figure 8). We also find that mean annual precipitation, land use, and soil characteristics emerge as important factors to classify drought indicator (Figure 9). The importance of topographic features and soil properties on drought vulnerability has been found by previous studies too [*Yeakley et al.*, 1998; *Miller and Poole*, 1983; *van Wesemael et al.*, 2003]. For example, *van Wesemael et al.* [2003] assess the impact of soil properties and topography on drought vulnerability for a rain-fed cropping system and show that both TWI and soil types play a significant role in determining drought states. For an experimental hill slope in southern Appalachian Mountains, US, *Yeakley et al.* [1998] show that topographic factors explain soil moisture variations during drier periods, while soil properties assert more control during wetter periods.

We have made few methodological choices that can be further improved in order to strengthen the results obtained here. First of all, land use change is simulated via a single parameter (fraction of deep rooted vegetation) in a lumped hydrologic model. It is well known that land use change has complex impacts on hydrologic characteristics and this rather simple representation is likely to limit the generality of our results related to vulnerability of indicators to land use change [*Costa et al.*, 2003; *Huang et al.*, 1999; *Li et al.*, 2009]. In addition, watersheds are heterogeneous systems and using a lumped model is likely to hide the potential diverse response within a watershed to change drivers. For example, *Mateus et al.* [2015] points out that the hydrologic sensitivity to climate change

varies with elevation even in a small watershed. Despite these model related limitations, the overall framework proposed here can accommodate more sophisticated hydrologic models, while keeping in mind that sampling strategies may need to accommodate larger run times.

In addition, the climate change scenarios adopted here only focus on changes in long term mean values of climatic variables while in reality watersheds around the world are undergoing change in both frequency and mean values of precipitation [*Van Oldenborgh et al.*, 2013]. Thus, a weather generator that allows us to sample different hydrologically relevant climatic characteristics such as duration of dry consecutive dry/wet days, frequency of wet/dry spells, in addition to the mean values of climate variables would be better suited to assess the vulnerability of watersheds to changing in characteristics of the climate [*Dullinger et al.*, 2004]. Also, the choice of hydrologic indicators used in this analysis was based on four broad ecologic, and economic indicators – availability of water, hydrologic extremes, and instream organisms, all calculable through a streamflow time series. Including habitat type and function will further strengthen this framework, but will require ecological models and/or socio-economic models to map environmental change to relevant indicators. As our main goal here is to present a framework that estimates model based vulnerability, the vulnerability metrics presented here provide examples of this process. Finally, although the present analysis shows a potential for regionalization of vulnerability indices, there is also a need to have detailed assessment of vulnerabilities of specific catchments that can lend further validity to this model based definition of vulnerability.

6. Conclusions

We present a method to quantify the vulnerability of a watershed to environmental change based on historical observations of its hydrologic response and physio-climatic characteristics. Our study provides a framework to understand the impact of climate and land use change on relevant hydrologic indicators independent of future projections of change drivers, thus aiding water systems managers to take decisions in the presence of large uncertainties. We also explore various definitions of vulnerability that describe average or extreme flow conditions, as well as others that are relevant from the point of view of instream organisms.

Our results indicate a potential mediation of climate change impacts by regional groundwater systems. We also find that controls on vulnerability vary based on the definition of the vulnerability indicator. For example, vulnerability indicator based on mean annual runoff shows a strong correlation with aridity index, while those based on extreme flows (flood and drought) do not. By implementing this analysis across a diverse range of watersheds in the conterminous US, we present a first of its kind quantification of vulnerability of watersheds of climate and land use change. Applying this analysis to a larger number of watersheds both in US and across the world may enable development of regional relationships between hydrologic indicator vulnerability to environmental change and watershed physio-climatic characteristics. Such regionalization of vulnerability metrics can also help in assessing vulnerability of ungauged basins to climate or land use change.

Acknowledgments. The data used in this analysis is described in Section 3 *Study area and data*. All the data are freely available for public use. Circos plots were made using *http* : *//circos.ca/*.

References

Addor, N., T. Ewen, L. Johnson, A. Çöltekin, C. Derungs, and V. Muccione (2015), From products to processes: Academic events to foster interdisciplinary and iterative dialogue in a changing climate, *Earth's Future*, *3*(8), 289–297.

Anandhi, A. A., N. N. Omani, I. Chaubey, R. Horton, D. Bader, and R. Nanjundiah (2015), What changes do the cmip5 climate models predict for south asia and what are some potential impacts on managed ecosystems and water resources, in *ASABE 1st Climate Change Symposium: Adaptation and Mitigation Conference Proceedings*, pp. 1–4, American Society of Agricultural and Biological Engineers.

Arnell, N. W. (2004), Climate change and global water resources: Sres emissions and socio-economic scenarios, *Global environmental change*, *14*(1), 31–52.

Asano, Y., and T. Uchida (2012), Flow path depth is the main controller of mean base flow transit times in a mountainous catchment, *Water Resources Research*, *48*(3).

Bai, Y., T. Wagener, and P. Reed (2009), A top-down framework for watershed model evaluation and selection under uncertainty, *Environmental Modelling & Software*, *24*(8), 901–916.

Bankes, S. (1993), Exploratory modeling for policy analysis, *Operations research*, *41*(3), 435–449.

Berghuijs, W. R., A. Hartmann, and R. A. Woods (2016), Streamflow sensitivity to water storage changes across europe, *Geophysical Research Letters*, *43*(5), 1980–1987.

624 Beven, K., and M. J. Kirkby (1979), A physically based, variable contributing area model
625 of basin hydrology/un modèle à base physique de zone d'appel variable de l'hydrologie
626 du bassin versant, *Hydrological Sciences Journal*, *24*(1), 43–69.

627 Blöschl, G. (2006), Hydrologic synthesis: Across processes, places, and scales, *Water*
628 *Resources Research*, *42*(3).

629 Blöschl, G. (2013), *Runoff prediction in ungauged basins: synthesis across processes, places*
630 *and scales*, Cambridge University Press.

631 Boso, F., F. Barros, A. Fiori, and A. Bellin (2013), Performance analysis of statistical
632 spatial measures for contaminant plume characterization toward risk-based decision
633 making, *Water Resources Research*, *49*(6), 3119–3132.

634 Bosshard, T., M. Carambia, K. Goergen, S. Kotlarski, P. Krahe, M. Zappa, and C. Schär
635 (2013), Quantifying uncertainty sources in an ensemble of hydrological climate-impact
636 projections, *Water Resources Research*, *49*(3), 1523–1536.

637 Brath, A., A. Montanari, and G. Moretti (2006), Assessing the effect on flood frequency
638 of land use change via hydrological simulation (with uncertainty), *Journal of Hydrology*,
639 *324*(1), 141–153.

640 Breiman, L., J. Friedman, C. J. Stone, and R. A. Olshen (1984), *Classification and re-*
641 *gression trees*, CRC press.

642 Brown, C., and R. L. Wilby (2012), An alternate approach to assessing climate risks, *Eos*,
643 *93*(41), 401–402.

644 Brown, C., W. Werick, W. Leger, and D. Fay (2011), A decision-analytic approach to
645 managing climate risks: Application to the upper great lakes1, *JAWRA Journal of the*
646 *American Water Resources Association*, *47*(3), 524–534.

Brown, C., Y. Ghile, M. Laverty, and K. Li (2012), Decision scaling: Linking bottom-up vulnerability analysis with climate projections in the water sector, *Water Resources Research*, *48*(9).

Brutsaert, W. (1993), Effective water table depth to describe initial conditions prior to storm rainfall in humid regions, *Water Resour. Res*, *29*, 427–434.

Chatterjee, S., A. Krishna, and A. Sharma (2014), Geospatial assessment of soil erosion vulnerability at watershed level in some sections of the upper subarnarekha river basin, jharkhand, india, *Environmental earth sciences*, *71*(1), 357–374.

Chen, C., S. Hagemann, and J. Liu (2015), Assessment of impact of climate change on the blue and green water resources in large river basins in china, *Environmental Earth Sciences*, *74*(8), 6381–6394.

Costa, M. H., A. Botta, and J. A. Cardille (2003), Effects of large-scale changes in land cover on the discharge of the tocantins river, southeastern amazonia, *Journal of Hydrology*, *283*(1), 206–217.

Dobler, C., S. Hagemann, R. Wilby, and J. Stötter (2012), Quantifying different sources of uncertainty in hydrological projections in an alpine watershed, *Hydrology and Earth System Sciences*, *16*(11), 4343–4360.

Duan, Q., J. Schaake, V. Andreassian, S. Franks, G. Goteti, H. Gupta, Y. Gusev, F. Habets, A. Hall, L. Hay, et al. (2006), Model parameter estimation experiment (mopex): An overview of science strategy and major results from the second and third workshops, *Journal of Hydrology*, *320*(1), 3–17.

Dullinger, S., T. Dirnböck, and G. Grabherr (2004), Modelling climate change-driven treeline shifts: relative effects of temperature increase, dispersal and invasibility, *Journal*

of ecology, *92*(2), 241–252.

Falcone, J. A., D. M. Carlisle, D. M. Wolock, and M. R. Meador (2010), Gages: A stream gage database for evaluating natural and altered flow conditions in the conterminous united states: Ecological archives e091-045, *Ecology*, *91*(2), 621–621.

Falkenmark, M., T. Chapman, et al. (1989), *Comparative hydrology: An ecological approach to land and water resources*, The Unesco Press.

Farmer, D., M. Sivapalan, and C. Jothityangkoon (2003), Climate, soil, and vegetation controls upon the variability of water balance in temperate and semiarid landscapes: Downward approach to water balance analysis, *Water Resources Research*, *39*(2).

Fraser, E. D., E. Simelton, M. Termansen, S. N. Gosling, and A. South (2013), vulnerability hotspots: Integrating socio-economic and hydrological models to identify where cereal production may decline in the future due to climate change induced drought, *Agricultural and Forest Meteorology*, *170*, 195–205.

Giuntoli, I., J. Vidal, C. Prudhomme, and D. Hannah (2015), Future hydrological extremes: the uncertainty from multiple global climate and global hydrological models, *Earth System Dynamics*, *6*(1), 267.

Gupta, S. C., A. C. Kessler, M. K. Brown, and F. Zvomuya (2015), Climate and agricultural land use change impacts on streamflow in the upper midwestern united states, *Water Resources Research*, *51*(7), 5301–5317.

Henderson, J., C. Rodgers, R. Jones, J. Smith, K. Strzepek, and J. Martinich (2015), Economic impacts of climate change on water resources in the coterminous united states, *Mitigation and Adaptation Strategies for Global Change*, *20*(1), 135–157.

692 Hidalgo, H. G., M. D. Dettinger, and D. R. Cayan (2008), Downscaling with constructed
693 analogues: Daily precipitation and temperature fields over the united states, *California*
694 *Energy Commission PIER Final Project Report CEC-500-2007-123*.
695 Huang, M., S. Kang, and Y. Li (1999), A comparison of hydrological behaviors of for-
696 est and grassland watersheds in gully region of the loess plateau, *Journal of Natural*
697 *Resources*, *14*(3), 226–231.
698 Johnson, T., J. Butcher, D. Deb, M. Faizullabhoy, P. Hummel, J. Kittle, S. McGinnis,
699 L. Mearns, D. Nover, A. Parker, et al. (2015), Modeling streamflow and water quality
700 sensitivity to climate change and urban development in 20 us watersheds, *JAWRA*
701 *Journal of the American Water Resources Association*, *51*(5), 1321–1341.
702 Kalantari, Z., A. Nickman, S. W. Lyon, B. Olofsson, and L. Folkeson (2014), A method for
703 mapping flood hazard along roads, *Journal of environmental management*, *133*, 69–77.
704 Kelleher, C., T. Wagener, B. McGlynn, A. Ward, M. Gooseff, and R. Payn (2013), Identifi-
705 ability of transient storage model parameters along a mountain stream, *Water Resources*
706 *Research*, *49*(9), 5290–5306.
707 Khader, A., D. E. Rosenberg, and M. McKee (2013), A decision tree model to estimate the
708 value of information provided by a groundwater quality monitoring network, *Hydrology*
709 *and Earth System Sciences*, *17*(5), 1797–1807.
710 Klein, T., D. Yakir, N. Buchmann, and J. M. Grünzweig (2014), Towards an advanced as-
711 sessment of the hydrological vulnerability of forests to climate change-induced drought,
712 *New Phytologist*, *201*(3), 712–716.
713 Kollat, J., P. Reed, and T. Wagener (2012), When are multiobjective calibration trade-offs
714 in hydrologic models meaningful?, *Water Resources Research*, *48*(3).

Krzywinski, M., J. Schein, I. Birol, J. Connors, R. Gascoyne, D. Horsman, S. J. Jones, and M. A. Marra (2009), Circos: an information aesthetic for comparative genomics, *Genome research*, *19*(9), 1639–1645.

Kunreuther, H., G. Heal, M. Allen, O. Edenhofer, C. B. Field, and G. Yohe (2013), Risk management and climate change, *Nature Climate Change*, *3*(5), 447–450.

Legesse, D., C. Vallet-Coulomb, and F. Gasse (2003), Hydrological response of a catchment to climate and land use changes in tropical africa: case study south central ethiopia, *Journal of Hydrology*, *275*(1), 67–85.

Lempert, R. J., B. P. Bryant, and S. C. Bankes (2008), Comparing algorithms for scenario discovery, *RAND, Santa Monica*.

Li, Z., W.-z. Liu, X.-c. Zhang, and F.-l. Zheng (2009), Impacts of land use change and climate variability on hydrology in an agricultural catchment on the loess plateau of china, *Journal of hydrology*, *377*(1), 35–42.

Mateus, C., D. D. Tullos, and C. G. Surfleet (2015), Hydrologic sensitivity to climate and land use changes in the santiam river basin, oregon, *JAWRA Journal of the American Water Resources Association*, *51*(2), 400–420.

Miller, P., and D. Poole (1983), The influence of annual precipitation, topography, and vegetative cover on soil moisture and summer drought in southern california, *Oecologia*, *56*(2-3), 385–391.

Moody, P., and C. Brown (2013), Robustness indicators for evaluation under climate change: Application to the upper great lakes, *Water Resources Research*, *49*(6), 3576–3588.

737 Nalbantis, I., and G. Tsakiris (2009), Assessment of hydrological drought revisited, *Water*
738 *Resources Management*, *23*(5), 881–897.

739 Nash, L. L., and P. H. Gleick (1991), Sensitivity of streamflow in the colorado basin to
740 climatic changes, *Journal of hydrology*, *125*(3), 221–241.

741 Nazemi, A. A., and H. S. Wheater (2014), Assessing the vulnerability of water supply
742 to changing streamflow conditions, *Eos, Transactions American Geophysical Union*,
743 *95*(32), 288–288.

744 Olden, J. D., and N. Poff (2003), Redundancy and the choice of hydrologic indices for
745 characterizing streamflow regimes, *River Research and Applications*, *19*(2), 101–121.

746 Poff, N. L., B. D. Richter, A. H. Arthington, S. E. Bunn, R. J. Naiman, E. Kendy,
747 M. Acreman, C. Apse, B. P. Bledsoe, M. C. Freeman, et al. (2010), The ecological limits
748 of hydrologic alteration (eloha): a new framework for developing regional environmental
749 flow standards, *Freshwater Biology*, *55*(1), 147–170.

750 Poff, N. L., C. M. Brown, T. E. Grantham, J. H. Matthews, M. A. Palmer, C. M. Spence,
751 R. L. Wilby, M. Haasnoot, G. F. Mendoza, K. C. Dominique, et al. (2015), Sustain-
752 able water management under future uncertainty with eco-engineering decision scaling,
753 *Nature Climate Change*.

754 Price, K. (2011), Effects of watershed topography, soils, land use, and climate on baseflow
755 hydrology in humid regions: A review, *Progress in physical geography*, *35*(4), 465–492.

756 Renner, M., R. Seppelt, and C. Bernhofer (2012), Evaluation of water-energy balance
757 frameworks to predict the sensitivity of streamflow to climate change, *Hydrology and*
758 *Earth System Sciences*, *16*(5), 1419–1433.

Reynard, N. S., C. Prudhomme, and S. M. Crooks (2001), The flood characteristics of large uk rivers: potential effects of changing climate and land use, *Climatic change*, *48*(2-3), 343–359.

Richter, B. D., J. V. Baumgartner, J. Powell, and D. P. Braun (1996), A method for assessing hydrologic alteration within ecosystems, *Conservation biology*, *10*(4), 1163–1174.

Ries, K. G. (1997), *August median streamflows in Massachusetts*, US Department of the Interior, US Geological Survey.

Rougé, C., J.-D. Mathias, and G. Deffuant (2015), Vulnerability: From the conceptual to the operational using a dynamical system perspective, *Environmental Modelling & Software*, *73*, 218–230.

Sankarasubramanian, A., R. M. Vogel, and J. F. Limbrunner (2001), Climate elasticity of streamflow in the united states, *Water Resources Research*, *37*(6), 1771–1781.

Sawicz, K. A. (2013), *Catchment classification-understanding hydrologic similarity through catchment function*, THE PENNSYLVANIA STATE UNIVERSITY.

Schaake, J., and C. Liu (1989), Development and application of simple water balance models to understand the relationship between climate and water resources, *New Directions for Surface Water Modeling*.

Schewe, J., J. Heinke, D. Gerten, I. Haddeland, N. W. Arnell, D. B. Clark, R. Dankers, S. Eisner, B. M. Fekete, F. J. Colón-González, et al. (2014), Multimodel assessment of water scarcity under climate change, *Proceedings of the National Academy of Sciences*, *111*(9), 3245–3250.

781 Schilling, K. E. (2016), Comment on climate and agricultural land use change impacts
782 on streamflow in the upper midwestern united states by gupta et al., *Water Resources*
783 *Research*.

784 Schottler, S. P., J. Ulrich, P. Belmont, R. Moore, J. Lauer, D. R. Engstrom, and J. E. Al-
785 mendinger (2014), Twentieth century agricultural drainage creates more erosive rivers,
786 *Hydrological processes*, *28*(4), 1951–1961.

787 Singh, R., T. Wagener, K. v. Werkhoven, M. Mann, and R. Crane (2011), A trading-
788 space-for-time approach to probabilistic continuous streamflow predictions in a chang-
789 ing climate–accounting for changing watershed behavior, *Hydrology and Earth System*
790 *Sciences*, *15*(11), 3591–3603.

791 Singh, R., T. Wagener, R. Crane, M. Mann, and L. Ning (2014a), A vulnerability driven
792 approach to identify adverse climate and land use change combinations for critical
793 hydrologic indicator thresholds: Application to a watershed in pennsylvania, usa, *Water*
794 *Resources Research*, *50*(4), 3409–3427.

795 Singh, R., S. Archfield, and T. Wagener (2014b), Identifying dominant controls on hydro-
796 logic parameter transfer from gauged to ungauged catchments–a comparative hydrology
797 approach, *Journal of Hydrology*, *517*, 985–996.

798 Sivapalan, M. (2009), The secret to doing better hydrological science: change the question!,
799 *Hydrological Processes*, *23*(9), 1391–1396.

800 Stewart, I. T. (2013), Connecting physical watershed characteristics to climate sensitivity
801 for california mountain streams, *Climatic change*, *116*(1), 133–148.

802 Sun, G., S. G. McNulty, J. M. Myers, and E. C. Cohen (2008), Impacts of climate change,
803 population growth, land use change, and groundwater availability on water supply and

demand across the conterminous us, *AWRA Hydrology & Watershed Management Technical Committee*.

Tebaldi, C., R. L. Smith, D. Nychka, and L. O. Mearns (2005), Quantifying uncertainty in projections of regional climate change: A bayesian approach to the analysis of multimodel ensembles, *Journal of Climate*, *18*(10), 1524–1540.

Teutschbein, C., and J. Seibert (2012), Bias correction of regional climate model simulations for hydrological climate-change impact studies: Review and evaluation of different methods, *Journal of Hydrology*, *456*, 12–29.

Therneau, T. M., B. Atkinson, and B. Ripley (2010), rpart: Recursive partitioning. r package version 3.1-46, *Computer software program retrieved from http://CRAN. R-project. org/package= rpart*.

Van Oldenborgh, G., M. Collins, J. Arblaster, J. Christensen, J. Marotzke, S. Power, M. Rummukainen, and T. Zhou (2013), Annex i: atlas of global and regional climate projections, *Climate change*, pp. 1311–1393.

Van Vliet, M. T., J. R. Yearsley, F. Ludwig, S. Vögele, D. P. Lettenmaier, and P. Kabat (2012), Vulnerability of us and european electricity supply to climate change, *Nature Climate Change*, *2*(9), 676–681.

van Werkhoven, K., T. Wagener, P. Reed, and Y. Tang (2008), Characterization of watershed model behavior across a hydroclimatic gradient, *Water Resources Research*, *44*(1).

van Wesemael, B., E. Cammeraat, M. Mulligan, and S. Burke (2003), The impact of soil properties and topography on drought vulnerability of rainfed cropping systems in southern spain, *Agriculture, ecosystems & environment*, *94*(1), 1–15.

827 Vetter, T., S. Huang, V. Aich, T. Yang, X. Wang, V. Krysanova, and F. Hattermann
828 (2015), Multi-model climate impact assessment and intercomparison for three large-
829 scale river basins on three continents, *Earth System Dynamics*, *6*(1), 17.

830 Vörösmarty, C. J., P. Green, J. Salisbury, and R. B. Lammers (2000), Global water
831 resources: vulnerability from climate change and population growth, *science*, *289*(5477),
832 284–288.

833 Watts, G., R. W. Battarbee, J. P. Bloomfield, J. Crossman, A. Daccache, I. Durance,
834 J. A. Elliott, G. Garner, J. Hannaford, D. M. Hannah, et al. (2015), Climate change
835 and water in the uk–past changes and future prospects, *Progress in Physical Geography*,
836 *39*(1), 6–28.

837 Weaver, C. P., R. J. Lempert, C. Brown, J. A. Hall, D. Revell, and D. Sarewitz (2013),
838 Improving the contribution of climate model information to decision making: the value
839 and demands of robust decision frameworks, *Wiley Interdisciplinary Reviews: Climate*
840 *Change*, *4*(1), 39–60.

841 Wood, A. W., L. R. Leung, V. Sridhar, and D. Lettenmaier (2004), Hydrologic implica-
842 tions of dynamical and statistical approaches to downscaling climate model outputs,
843 *Climatic change*, *62*(1-3), 189–216.

844 Yeakley, J. A., W. Swank, L. Swift, G. Hornberger, and H. Shugart (1998), Soil mois-
845 ture gradients and controls on a southern appalachian hillslope from drought through
846 recharge, *Hydrology and Earth System Sciences Discussions*, *2*(1), 41–49.

847 Zhao, F. L., Zhang, and Zhang (1980), The xinanjiang model, in proceedings of the
848 symposium on the application of recent developments in hydrological.

Table 1. Description of hydrologic model parameters

	Parameter	Description	Feasible range lower	upper	Units
Soil	Sb	Maximum depth of soil store	0	2000	mm
	B	Shape factor of distribution bucket	0	7	[-]
	Fc	Threshold storage parameter	0	1	[-]
	Kd	Deep recharge coefficient from the upper saturated zone to the deep store	0	0.5	[-]
Vegetation	% Veg	Fraction of watershed area covered by deep rooted vegetation	0	1	[-]
	LAImax	Maximum Leaf Area Index	0	6	mm
	LAImin	Minimum Leaf Area Index	0	6	mm
	Cei	Maximum canopy interception	0	0.49	mm
Routing	A_{SS}	Recession coefficient for saturated soil	0.05	0.5	day^{-1}
	A_{BF}	Recession coefficient for groundwater	0.001	0.05	day^{-1}
Snow	Ddf	Degree day factor	0	20	$mm\,°C^{-1}\,day^{-1}$
	Tth	Threshold factor for snow formation	-5	5	°C
	Tb	Base temperature for snow melt	-5	5	°C

Table 2. Description and class definitions for hydrologic indicators used in the study

No.	Indicator	Description	Class definition
1	Mean annual runoff	Mean annual runoff normalized by watershed area *Olden and Poff* [2003]	Change in streamflow C0: >0% C1: 0% to -25% C2: -25% to -50% C3: <-50%
2	Flood	Mean number of high flow events per year using an upper threshold of 3 times median flow over all years *Olden and Poff* [2003]	Frequency of flood C0: <0% C1: 0% to 25% C2: 25% to 50% C3: >50%
3	IQ_{dsc}	Proportion of index flow removed where index flow is median August flow divided by mean annual flow [*Poff et al.*, 2010]	Index flow decreased C0: <0.2 C1: 0.2 to 0.4 C2: >0.4
4	Drought	Streamflow Drought Index (SDI) [*Nalbantis and Tsakiris*, 2009]	Based on ranges of SDI C0: SDI $\geq$0.0 C1: -1.0 $\leq$ SDI <0.0 C2: -1.5 $\leq$ SDI <1.0 C3: -2.0 $\leq$ SDI <1.5 C4: <-2.0

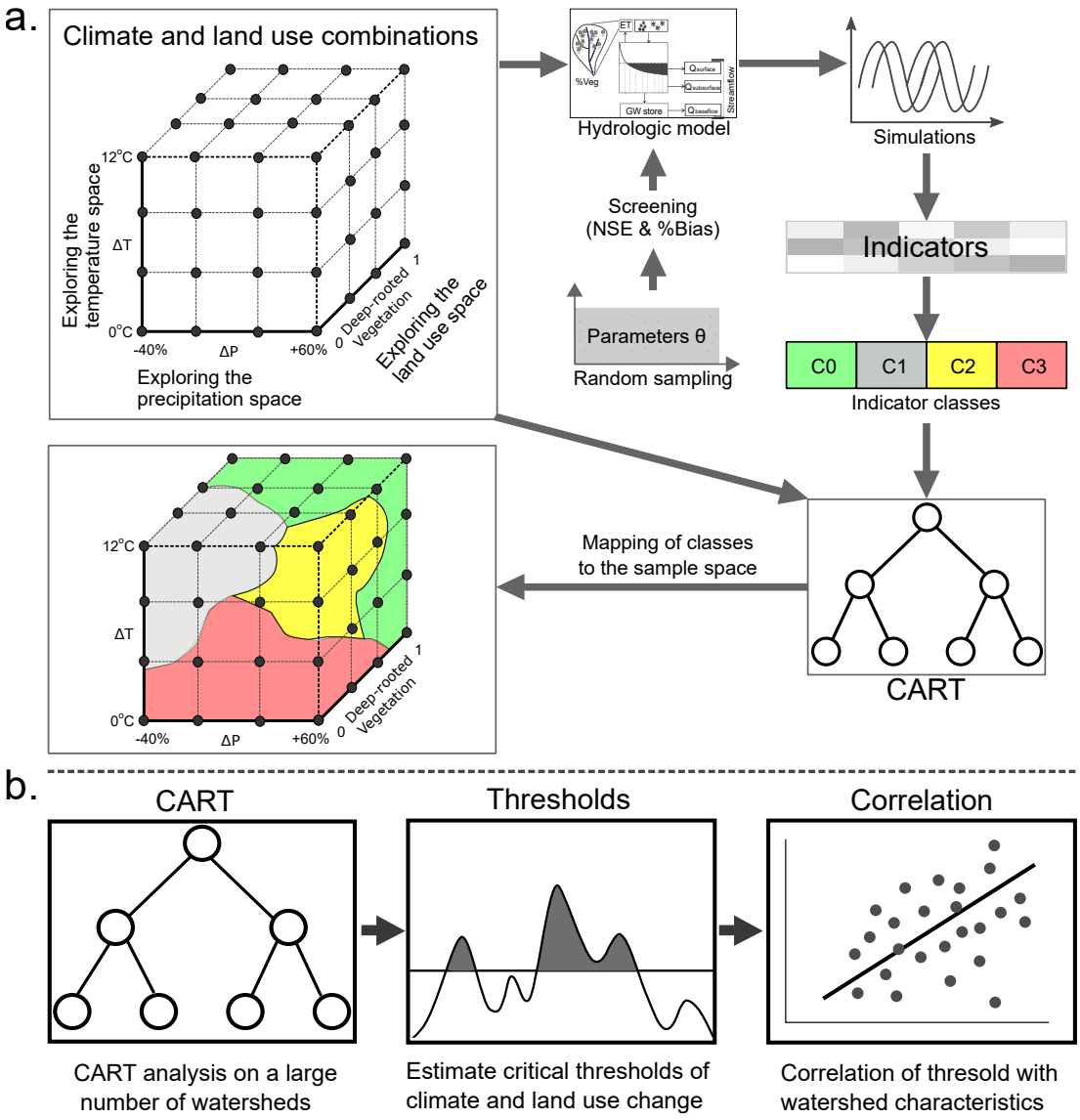

Figure 1. The exploratory modelling framework to estimate vulnerability and its dependence on watershed's physio-climatic characteristics. (a) A large range of climate and land use change combinations are generated and then used to simulate runoff using a hydrological model while accounting for parametric uncertainty. Next, hydrologic indicators are calculated based on the simulated flow and classified into different vulnerability classes. Finally, CART algorithm estimates critical climate change and land use thresholds. (b) Applying comparative hydrology approach by correlating critical climate change and land use thresholds with watershed physio-climatic characteristics.

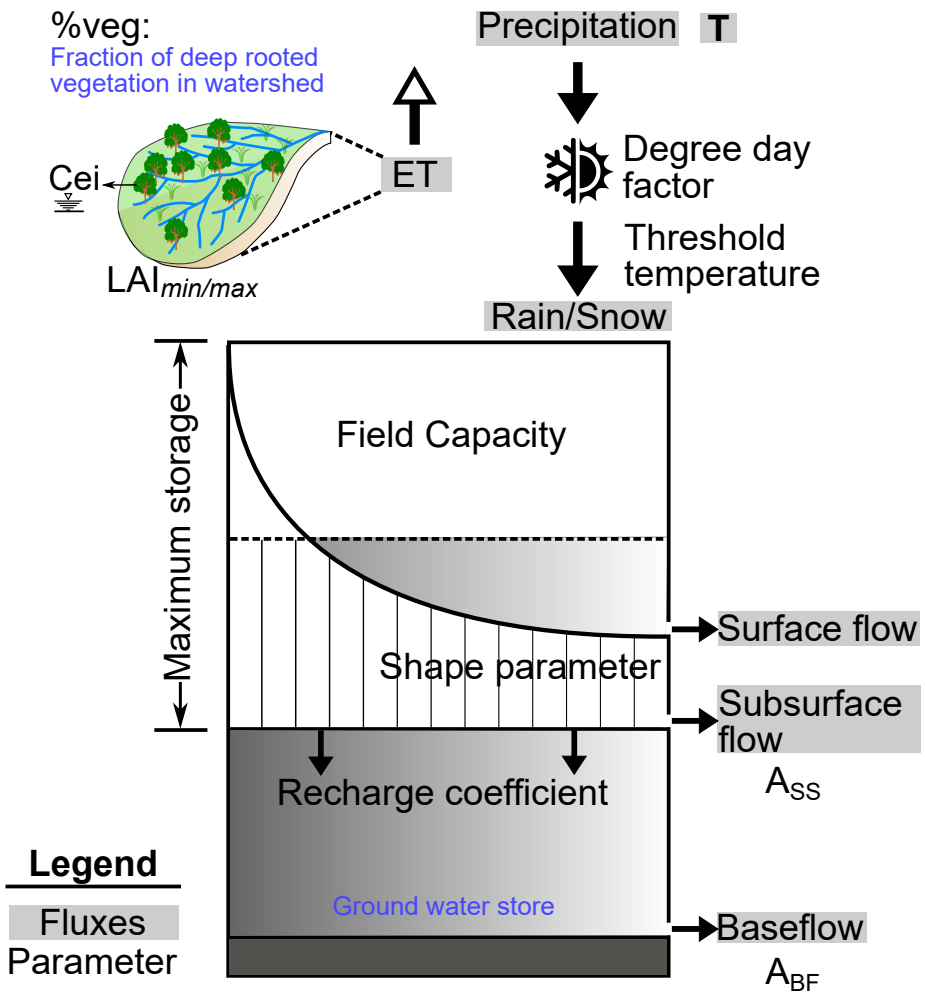

Figure 2. The parsimonious hydrologic model structure used in the study. Land use is incorporated as percentage of deep rooted vegetation in the watershed.

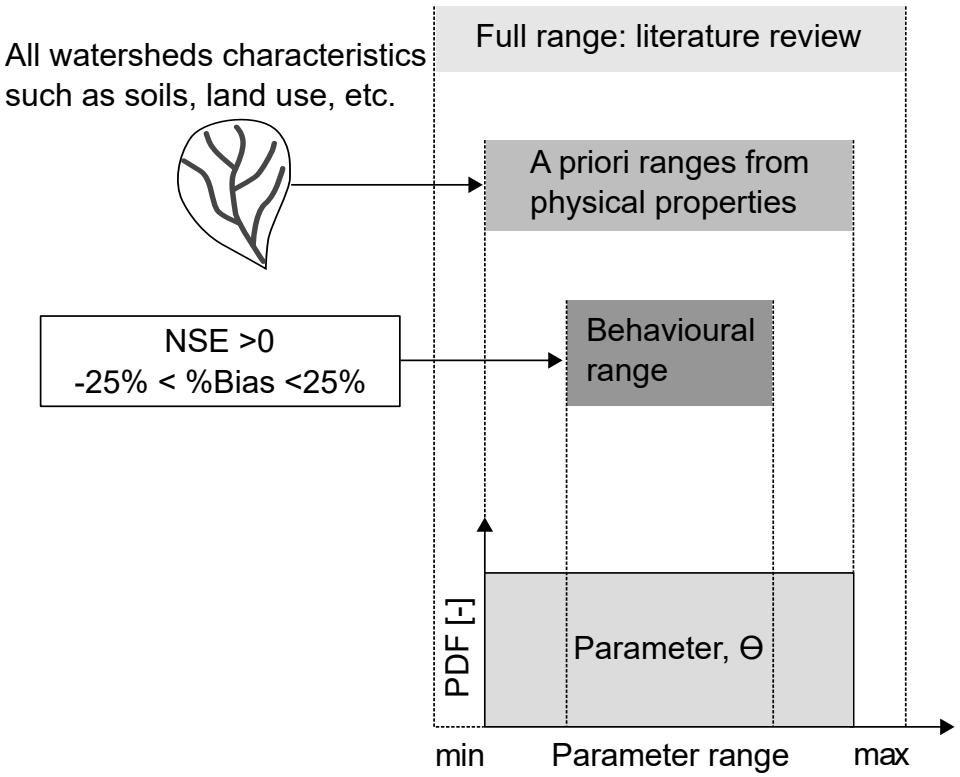

Figure 3. Incorporating parametric uncertainty in the exploratory modelling framework. First, a wide range of possible values is fixed for each parameter based on literature review. Next, *a priori* parameter ranges are estimated using watershed's physical characteristics for selected parameters. Finally, the behavioural range of parameters is arrived at using NSE and percentage Bias criteria.

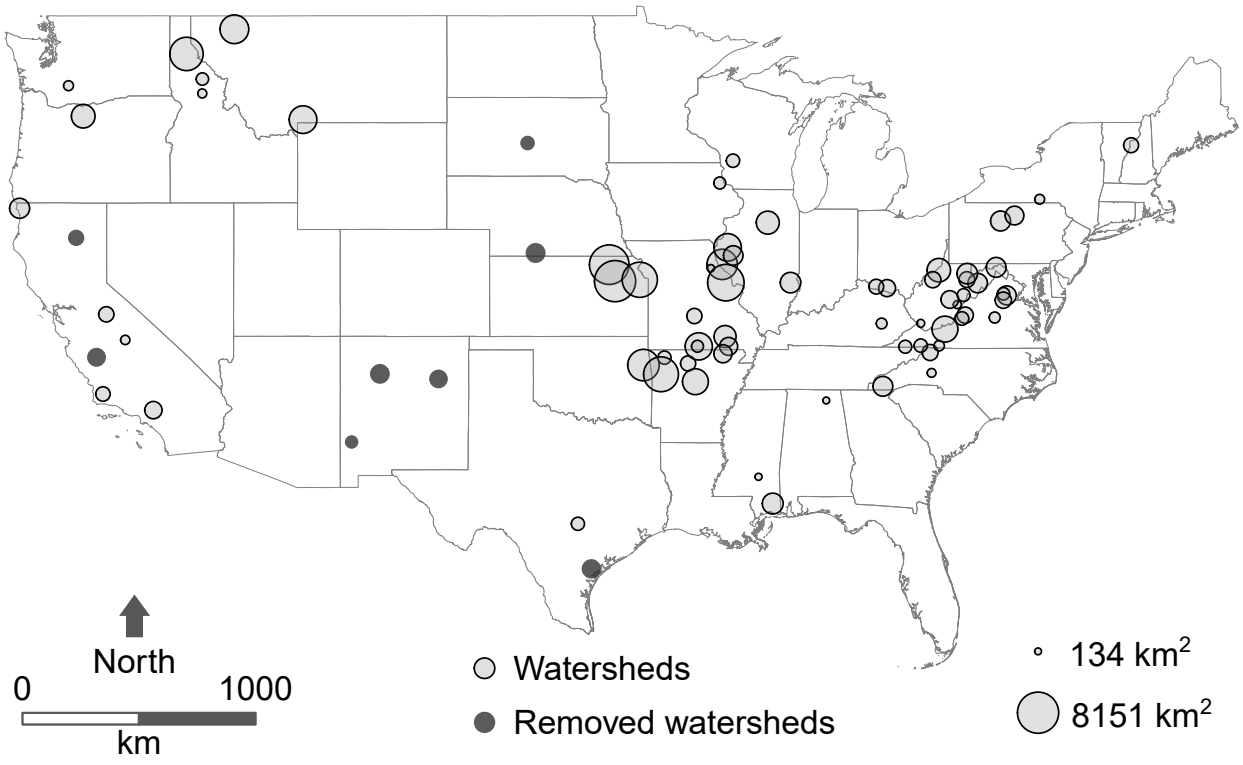

Figure 4. Location of the watersheds used in the study. Each circle on the map represents the centroid of the watershed, and size of each circle represents the watershed area. Watersheds represented by solid black filled circles are removed from the analysis due to low runoff ratios (<0.1) or low model performance.

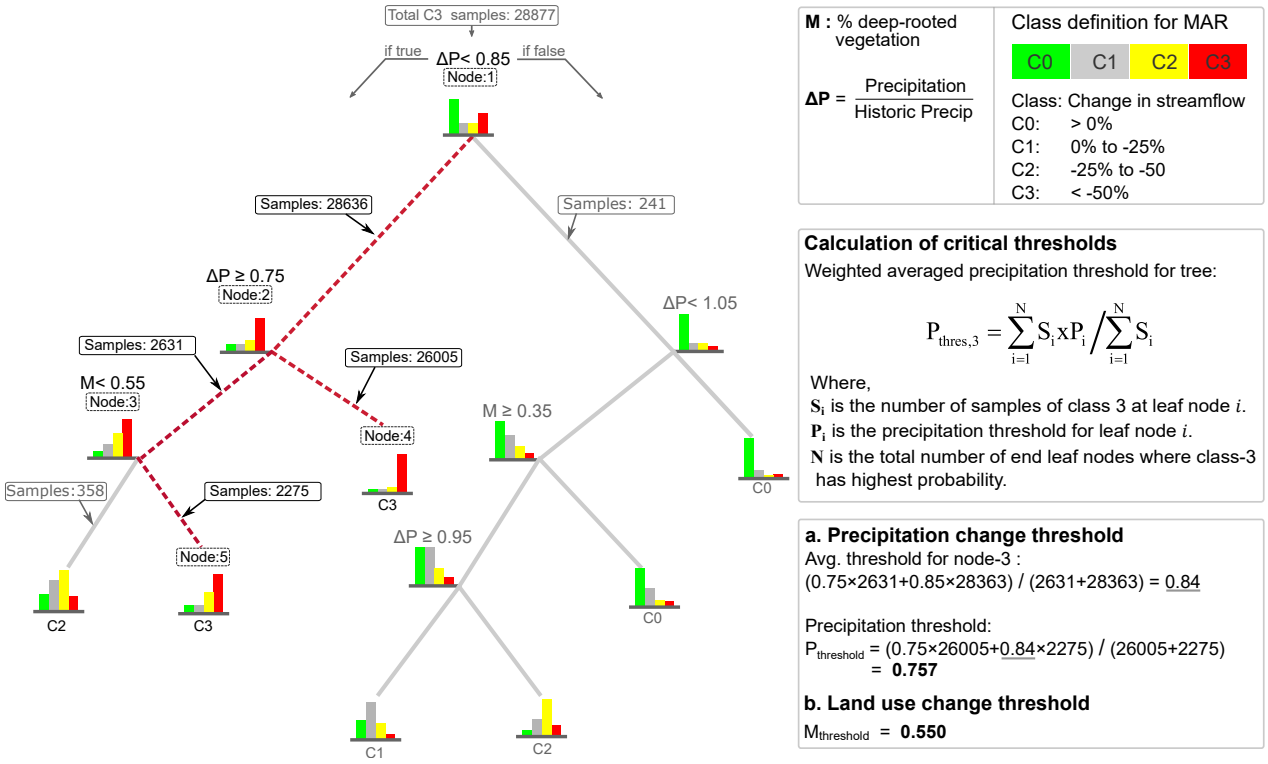

Figure 5. Computation of critical precipitation change and land use thresholds using CART. The thresholds are calculated based on weighted averaged of the threshold values on leaf (end) nodes that lead to vulnerability classes. A typical output from CART algorithm for a watershed–indicator (mean annual runoff) combination is shown. Red color bars denote highest vulnerability class (C3) and red dashed line represents the paths leading to C3 for a watershed.

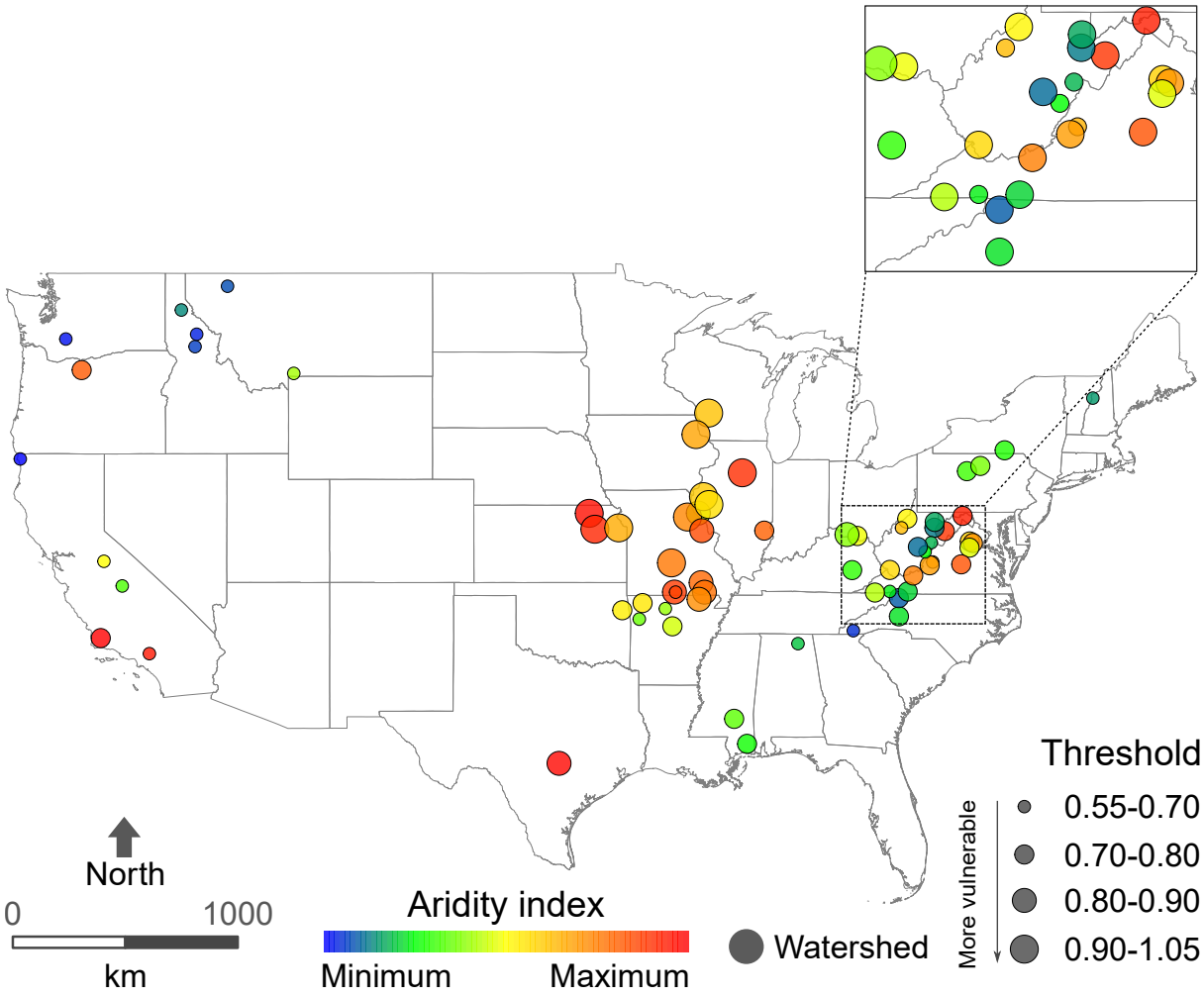

Figure 6. Spatial distribution of critical precipitation change thresholds that lead to the highest class of vulnerability (C3) for water availability, represented by long term mean annual runoff. Each watershed is represented by a circle, where size corresponds to the threshold value, and color denotes aridity index (ratio of long term potential evapotranspiration to long term precipitation.

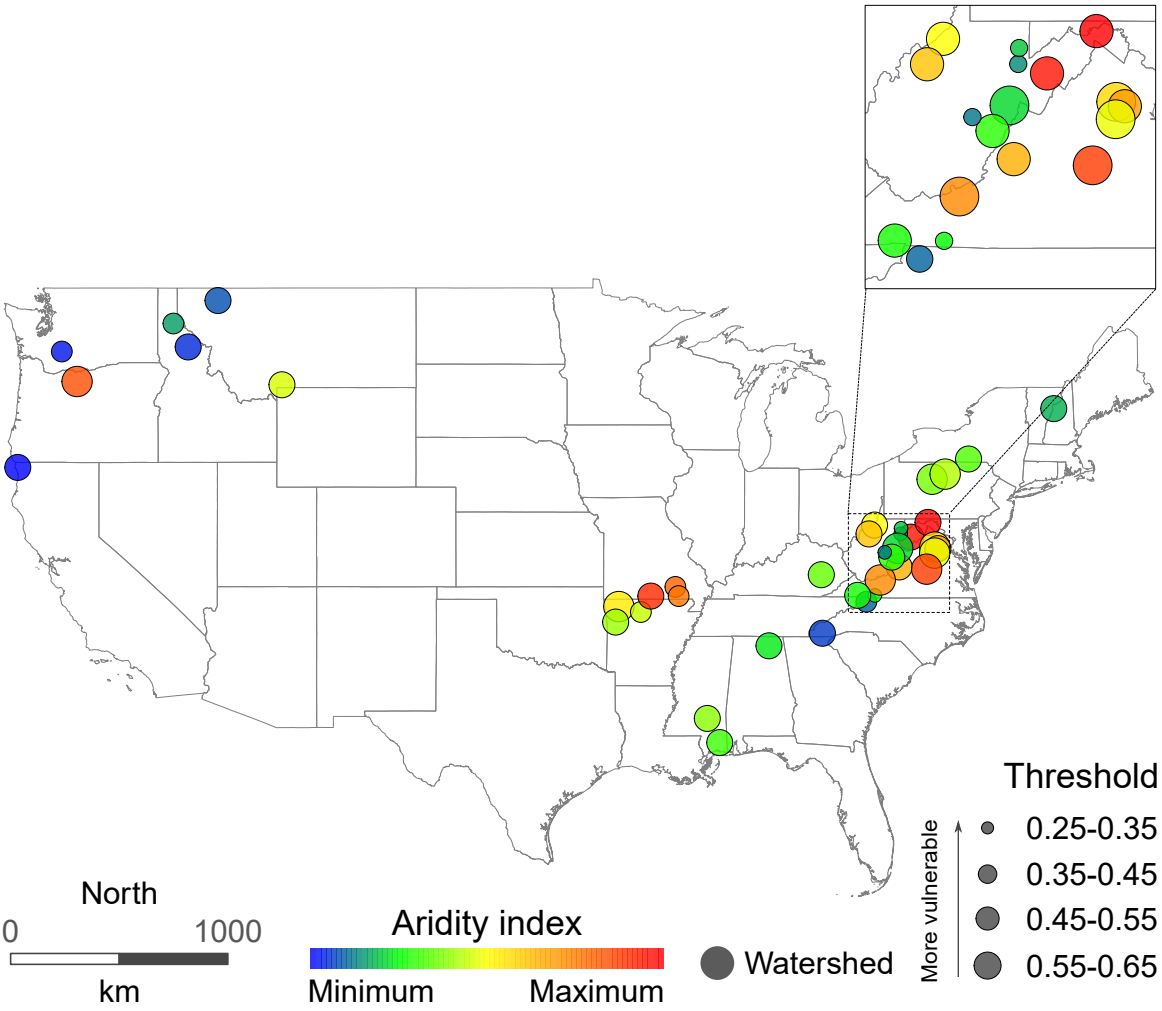

Figure 7. Spatial distribution of critical land use thresholds that lead to the highest class of vulnerability (C3) for water availability. The color and size of circles denote the same variables as Figure 6.

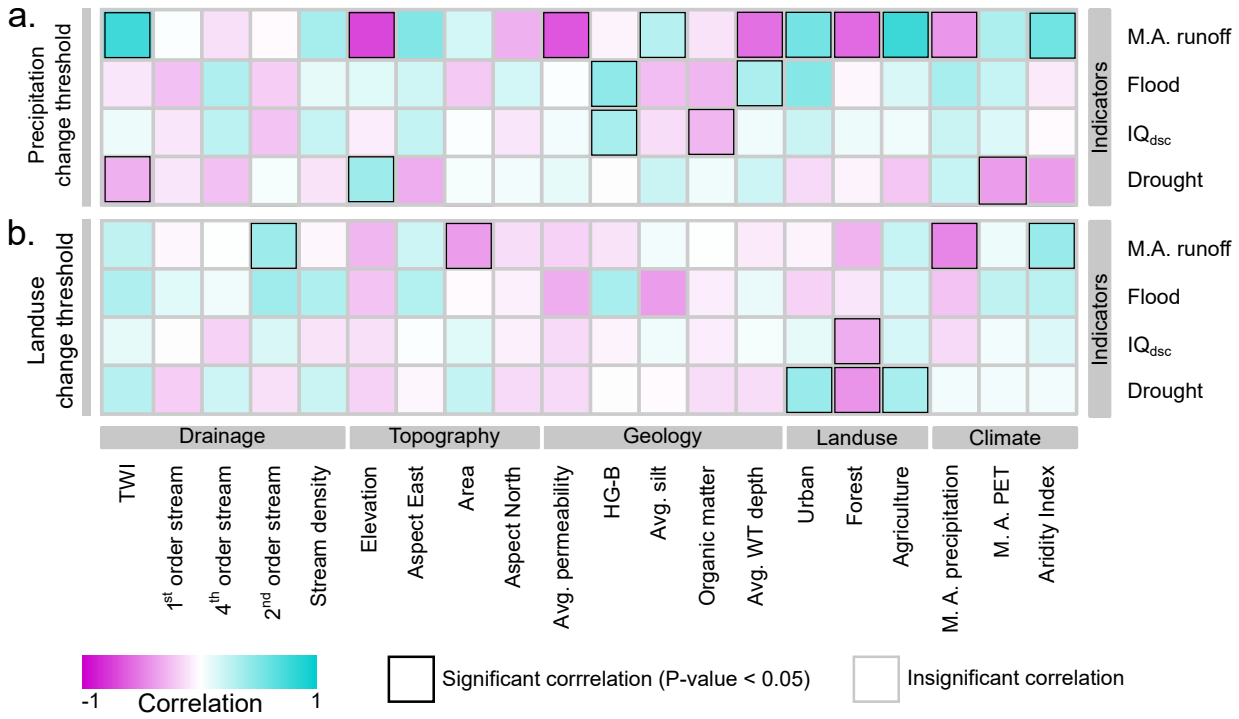

Figure 8. Correlation between watershed characteristics and critical thresholds for (a) precipitation change, and (b) land use. Indicators are displayed in rows and watershed characteristics in columns. Color represents the strength of the correlation and black borders highlight significant correlations.

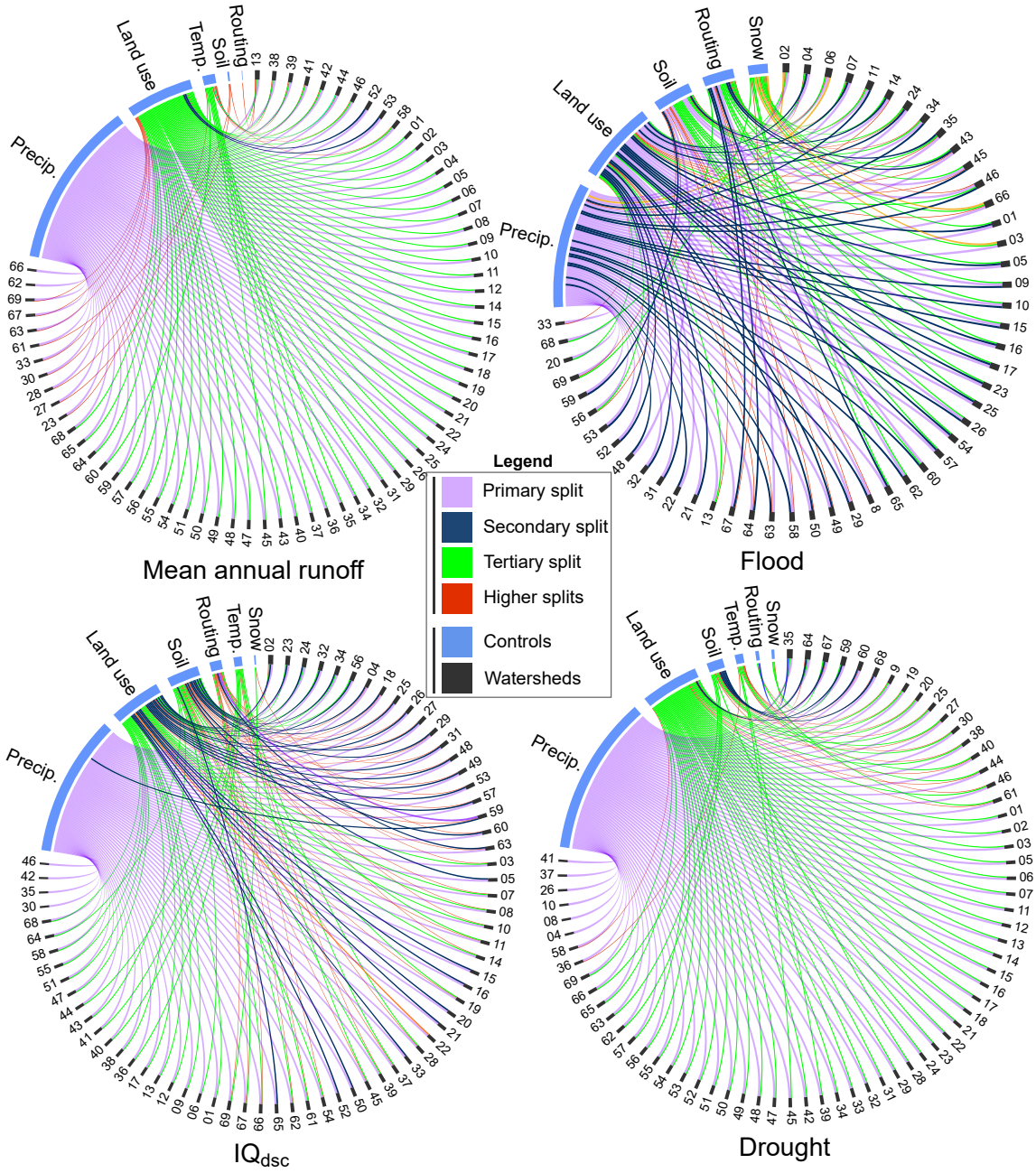

Figure 9. Circos plots to visualize dominant controls for each indicator–watershed combination. Each circos plot represents one indicator. Outer edges of the plot show different controls on indicator value as identified by CART and all watersheds represented by their serial numbers. Purple, blue, green, and red lines connecting watershed controls and serial number, indicate a decreasing level of importance.